Neuro-Oncology

22(9), 1289–1301, 2020 | doi:10.1093/neuonc/noaa051 | Advance Access date 30 March 2020

Actinomycin D downregulates Sox2 and improves survival in preclinical models of recurrent glioblastoma

Jessica T. Taylor, Stuart Ellison, Alina Pandele, Shaun Wood, Erica Nathan, Gabriella Forte, Helen Parker, Egor Zindy, Mark Elvin, Alan Dickson, Kaye J. Williams, Konstantina Karabatsou, Martin McCabe, Catherine McBain, and Brian W. Bigger

Brain Tumor Research Group, Stem Cell and Neurotherapies Laboratory, Division of Cell Matrix Biology and Regenerative Medicine, University of Manchester, Manchester, UK (J.T.T., A.P., G.F., H.P., B.W.B.); Faculty of Biology, Medicine and Health, University of Manchester, Manchester, UK (E.Z.); Manchester Institute of Biotechnology, Faculty of Science and Engineering, University of Manchester, Manchester, UK (M.E., A.D.); CRUK Cambridge Institute, Li Ka Shing Centre, Cambridge, UK (E.N.); Department of Neurosurgery, Salford Royal Hospital NHS Foundation Trust, Manchester, UK (K.K.); Division of Pharmacy and Optometry, School of Biology, Medicine and Health, University of Manchester, Manchester, UK (K.J.W.); Division of Cancer Sciences, University of Manchester, Manchester, UK (M.M.); Department of Clinical Oncology, The Christie NHS FT, Manchester, UK (C.M.)

Corresponding Author: Professor Brian W Bigger, Stem Cell and Neurotherapies Laboratory 3.721 Stopford Building, University of Manchester, United Kingdom, M13 9PT (brian.bigger@manchester.ac.uk)

Abstract

Background. Glioblastoma (GBM) has been extensively researched over the last few decades, yet despite aggressive multimodal treatment, recurrence is inevitable and second-line treatment options are limited. Here, we demonstrate how high-throughput screening (HTS) in multicellular spheroids can generate physiologically relevant patient chemosensitivity data using patient-derived cells in a rapid and cost-effective manner. Our HTS system identified actinomycin D (ACTD) to be highly cytotoxic over a panel of 12 patient-derived glioma stemlike cell (GSC) lines. ACTD is an antineoplastic antibiotic used in the treatment of childhood cancers. Here, we validate ACTD as a potential repurposed therapeutic for GBM in 3-dimensional GSC cultures and patient-derived xenograft models of recurrent glioblastoma.

Methods. Twelve patient-derived GSC lines were screened at 10 μM, as multicellular spheroids, in a 384-well serum-free assay with 133 FDA-approved compounds. GSCs were then treated in vitro with ACTD at established half-maximal inhibitory concentrations (IC_{50}). Downregulation of sex determining region Y–box 2 (Sox2), a stem cell transcription factor, was investigated via western blot and through immunohistological assessment of murine brain tissue.

Results. Treatment with ACTD was shown to significantly reduce tumor growth in 2 recurrent GBM patient-derived models and significantly increased survival. ACTD is also shown to specifically downregulate the expression of Sox2 both in vitro and in vivo.

Conclusion. These findings indicate that, as predicted by our HTS, ACTD could deplete the cancer stem cell population within the tumor mass, ultimately leading to a delay in tumor progression.

Key Points

1. High-throughput chemosensitivity data demonstrated the broad efficacy of actinomycin D, which was validated in 3 preclinical models of glioblastoma.
2. Actinomycin D downregulated Sox2 in vitro and in vivo, indicating that this agent could target the stem cell population of GBM tumors.

Importance of the Study

Glioblastoma is a highly aggressive and devastating disease, yet no standard of care exists after recurrence following first-line therapy. Using 3D multicellular spheroid HTS, we identify ACTD as a potent cytotoxic agent against GSCs from 12 patients. We demonstrate that treatment with ACTD in preclinical models of recurrent GBM gives a significant increase in survival and downregulates the transcription factor Sox2 at low concentrations. Through fast and reproducible HTS and robust validation in vivo, this study indicates the potential of ACTD as a potent and effective option at recurrence for GBM patients in the clinic.

The most common primary adult brain tumor, glioblastoma multiforme (GBM), is also one of the most well characterized.[1] Despite a huge increase in the scientific understanding of this devastating disease, therapeutic options for GBM still remain limited. Irrespective of the current aggressive and multimodal first-line approach at diagnosis, consisting of maximal surgical resection, radiotherapy, and adjuvant chemotherapy with temozolomide (TMZ),[2] recurrence in GBM is practically an inevitability and there is currently no defined standard of care for patients who relapse.[3] With only a 3.4% probability of success for new oncology drugs coming through the pharmaceutical pipeline, compared with a 13.8% FDA-approval rate of all drug development campaigns,[4] the need for more innovative therapeutic strategies to expedite novel glioblastoma therapeutics is imperative.

At a cellular level, GBM is highly heterogeneous and comprises multiple subpopulations of distinct cell types, many of which express stem cell markers.[5] These glioma stemlike cells (GSCs) share many features of neural stem cells of the subventricular zone, including high motility and expression of markers such as Nestin and sex determining region Y–box 2 (Sox2).[6–8] They are also capable of self-renewal, initiate tumors in immunocompromised mouse models, and have been shown to be significantly more resistant to current therapeutic options for GBM.[9] Consequently, following first-line treatment, a resistant cancer stem cell population remains to drive tumor recurrence.[10]

Sox2 is an important regulator in the self-renewal of human embryonic stem cells, while also playing a role in stem cell maintenance in many adult tissues, including the brain.[11] Overexpression of Sox2 has been linked to the development of many solid tumors, such as lung, ovarian, and breast cancer, and has more recently become associated with GBM. High levels of Sox2 are associated with a worse prognosis, and patient tumors with increased Sox2 expression have been found to be more aggressive.[12–14] Knockdown of Sox2 has also been shown to decrease proliferation of GSCs and reduce migration and invasion, as well as causing a loss of tumorigenic potential in vivo.[15]

The plasticity of the tumor microenvironment, and the cells that reside within it, presents an enormous challenge to the development of novel therapies. Therapeutics that could potentially abrogate the oncogenic effects of Sox2 in GBM stemlike cells are therefore an interesting prospect, especially those that are already approved for alternative clinical applications such as ACTD. Work done previously in our group[16] has demonstrated that automated screening of repurposed drug libraries is feasible in clinically relevant time-frames, while revealing ACTD to be a potent cytotoxic agent in seven GSC lines. Here we use a refined screening process to confirm our findings in an additional 5 GSC lines and validate ACTD as a potential therapeutic for recurrent GBM in multiple patient-derived in vivo models.

Materials and Methods

Patient Cell Lines

Patients with GBM or recurrent GBM were identified via the neuro-oncology multidisciplinary meeting at Salford Royal NHS Foundation Trust and samples confirmed by a pathologist prior to cell line derivation. Patient demographics are summarized in Supplementary Table 1. Informed consent was obtained from patients for tissue use, storage, and derivation of cell lines. All work was performed under National Health Service (NHS) research ethics committee approval (Ref. 68/H1006/38 and 08/H1006/37). DNA for patient samples for lines TD1–3 and BK1 and BK3 was analyzed by the free online brain tumor classifier[17] at (www.molecularneuropathology.org) for methylation subgrouping. Patient lines GS1-TS20 are described further by Yu et al.[16]

Patient Cell Line Derivation and Cell Culture

Patient cell line derivation and expansion were performed as described[16] using serum-free methods. All cells were cultured in neurobasal medium (NBM) supplemented with 1x N-2 and 1x B-27 and growth factors epidermal growth factor and human fibroblast growth factor (20 ng/mL). Cells were maintained at 37°C, 5% CO_2 in ultra-low adherent flasks (Corning) as neurospheres and passaged weekly. DNA for cell lines TD1–3 and BK1 and BK3 were also subjected to methylation subgrouping at passage 5 to ensure they reflected the original patient samples. For invasion assays, spheroids were seeded in supplemented NBM in 96-well ultra-low attachment plates (Nunc) and allowed to form spheroids over 48 hours. Matrigel extracellular matrix–based hydrogel (Corning) was then added to wells, with or without drug. To assess GSC renewal, spheroids were seeded into 24-well low attachment plates (Corning). Five days after seeding, spheroids were counted, then drug treatment added. Spheroids were again counted 5 days post drug treatment, then left to recover for a further 5 days. Finally, spheroids were dissociated and re-seeded to assess self-renewal ability.

Lentiviral Labeling of Cell Lines

The pLenti CMV Puro LUC (w168–1) was a kind gift from Eric Campeau and Paul Kaufman (Addgene plasmid # 17477).[18] High-titer lentiviral particles were generated as previously described.[19] Luciferase-expressing patient-derived lines were established through stable transfection of the CMV Puro LUC lentivirus and subsequent puromycin selection.

Chemicals

The Approved Oncology Drugs Set VIII consisting of 133 FDA-approved chemotherapeutic drugs (Supplementary Data File 1) was kindly provided by the National Cancer Institute Division of Cancer Treatment and Diagnosis/Developmental Therapeutics Program (http://dtp.cancer.gov). Drugs were provided as 20 µL stocks at 10 mM in 100% dimethyl sulfoxide (DMSO) in 96-well polypropylene U-bottom plates (Greiner). Dilution stock plates were made up in 384-well polypropylene F-bottom microtiter plates (Corning) using the Biomek FX liquid handling platform (Beckman Coulter). Drugs for in vivo use were obtained from Sigma Aldrich.

In Vitro Drug Screening

Low-passage patient-derived cells, cultured in serum-free conditions, were plated using a Multidrop Combi liquid dispenser (ThermoFisher Scientific) into 384-well ultra-low attachment plates (Corning) and cultured for 24 hours to allow for robust spheroid formation. Approved Oncology Drugs Set VIII compounds were added to wells either as a single shot dose of 10 µM or in a 6-point dose response in duplicate using the Biomek FX liquid handling platform. Each experiment was carried out twice, with vehicle (5% DMSO) and cell death controls (25 µM benzethonium chloride).

After 96-hour incubation in a Cytomat 6000 carousel incubator, PrestoBlue or CellTiter-Glo 3D reagent (Promega) was added to wells at volumes recommended by the manufacturers using a Multidrop Combi. Cell viability was measured using a Synergy HT Multi-Detection Microplate Reader (BioTek) and dose-response curves and IC_{50} values calculated using GraphPad Prism v7.0.

In Vivo Studies

Nonobese diabetic severe combined immunodeficient gamma null (NSG) female mice between 8 and 12 weeks of age were used in this study. Mice were housed in groups of 2–5 in individually ventilated cages with ad libitum access to food and water and kept on a 12-hour light/dark cycle. All procedures were ethically approved by the University of Manchester Ethical Review Process under UK Home Office regulations and project licenses PPL 70/07760, 40/3658, and P0C3AEEBO. All drug concentrations used, dosing regimens. and methods of delivery are described in detail in Supplementary Table 2. DNA from implanted cell lines TS9 and TD2 (both luciferase and non-luciferase expressing) was also subjected to methylation subgrouping to ensure that in vivo studies reflected the original patient samples.

Subcutaneous Tumor Studies

Female NSG mice, aged ≥8 weeks, were implanted with subcutaneous flank xenografts using TS9 patient-derived recurrent GBM cells (1×10^7 per mouse). Palpable tumors were established approximately 6 weeks after cells were injected. Drug treatment was initiated when tumors reached 200 mm^3. Mice were culled when they reached humane endpoints including, but not limited to, a tumor volume of 800 mm^3. Tumors were excised and final tumor volumes were measured and plotted against controls.

Orthotopic Models

TD2 luciferase-expressing cells (2.5×10^5 per mouse) were stereotactically injected into the right striatum of NSG mice under aseptic conditions. Mice were imaged using the In-Vivo Xtreme Imaging System (Bruker) prior to treatment for randomization. Mice were treated with vehicle (5% DMSO), TMZ (140 mg/kg), or ACTD (0.1 mg/kg) according to the dosing schedule outlined in Supplementary Table 2, then reimaged. Mice were culled via transcardial perfusion of phosphate buffered saline under terminal anesthesia. Brains were harvested, fixed in 4% paraformaldehyde, and cryoprotected with 20% sucrose for histology.

For long-term survival analysis, a cohort of 25 mice were stereotactically injected with TD2 patient-derived cells (5×10^5 per mouse). Mice were randomized 6 weeks post-implantation, then treated with vehicle (5% DMSO), TMZ (140 mg/kg), low dose ACTD (0.05 mg/kg), or high dose ACTD (0.1 mg/kg) according to the dosing schedule outlined in Supplementary Table 2. Animals were monitored for signs of tumor burden including, but not limited to, weight loss of >20%, head tilt, domed head, or abnormal gait. When humane endpoints were reached, animals were culled and brains harvested for histological analysis. For western blot analysis, brains were flash-frozen in cold isopentane and homogenized in radioimmunoprecipitation assay buffer at –20°C before being processed appropriately.

Immunostaining

Whole spheroids were processed and imaged as described.[16] Briefly, spheroids were incubated with primary antibodies at the following dilutions: Nestin 1:1000 (Abcam) and Sox2 1:250 (Abcam). Secondary staining was performed using Alexa Fluor 488 and 594 secondary antibodies (Invitrogen), followed by nuclear counterstaining with 4′,6′-diamidino-2-phenylindole (DAPI) (300 mM).

Immunohistochemistry was performed on free-floating sections treated with 10% goat serum for 2 hours at room temperature, and then stained with primary antibodies for Nestin (10C2), 1:500 (ab22035, Abcam); Sox2, 1:100 (ab97959, Abcam); octamer-binding transcription factor 4 (Oct4), 1:200 (ab19857, Abcam); and glial fibrillary acidic protein, 1:1000 (ZO334, Dako). Primary antibodies were detected using the appropriate secondary antibodies, and

images were acquired on a 3D-Histech Pannoramic-250 microscope slide scanner using a 20 ×/ 0.30 Plan Achromat objective (Zeiss) and processed using Case Viewer software (3D-Histech).

Quantitative Real-Time PCR

Tumors were excised macroscopically and cells dissociated from untreated mice. Dissociated tumor cells were treated ex vivo with 0.1% DMSO or 10 nM ACTD for 24 hours and total RNA extracted. Complementary DNA was synthesized and reverse transcription quantitative PCR was performed on a CFX96 Real-Time PCR Detection System (BioRad) with TaqMan reagents (ThermoFisher) according to the manufacturer's recommended protocol. Gene expression was normalized to the expression of 18S. Detailed methods and reaction parameters can be found in the Supplementary Methods and Results.

Statistical Analysis

IC_{50} values were interpolated from sigmoidal dose-response curves with 95% confidence intervals. IC_{50} values were evaluated for statistical significance via unpaired *t*-test, with significance set at $P < 0.05$. Where 3 or more groups were compared, one-way or two-way ANOVA with drug treatment as a factor, followed by Tukey's multiple comparison test, was performed with significance set at $P < 0.05$. Survival was analyzed using Kaplan–Meier curves and log-rank (Mantel–Cox) tests. Error bars are represented by standard deviation unless otherwise stated. All statistical data analysis and curve fitting were performed using GraphPad Prism v8.

Hierarchical clustering was performed using the Morpheus matrix visualization and analysis software at https://software.broadinstitute.org/morpheus (Broad Institute).

Z′ factor values were calculated by measuring fluorescence or luminescence of replicate 0.1% DMSO vehicle-treated cells and 25 μM benzethonium chloride–treated cells on quality control plates and chemosensitivity plates as described.[20]

Results

High-Throughput Screening in Patient-Derived Glioma Stemlike Multicellular Spheroids Demonstrates Heterogeneity in Chemotherapeutic Response

Twelve patient-derived GSC lines were screened with the Approved Oncology Drugs Set VII at 10 μM (Fig. 1A). Cells were seeded in 384-well ultra-low attachment plates in supplemented NBM, which resulted in reproducible, multicellular spheroids within 12 hours (Supplementary Figure 1A). DMSO-treated (0.1%) and benzethonium chloride–treated (25 μM) cells were used as controls, and cell death was measured using the PrestoBlue assay 96 hours posttreatment. An orthogonal luciferase-based assay, CellTiter-Glo 3D, was used to exclude any potential interference from fluorescent drugs. Both assays were shown to be robust and reproducible, with Z′ values well above 0.5, indicating a high-quality screen (Supplementary Figures 2–5). The immortalized cell line U87 was also seeded in serum-free media and screened alongside patient-derived lines for comparison.

Hierarchical clustering of chemotherapeutic response in the PrestoBlue HTS assay demonstrated that no specific drug classes produced consistent cell death across all GSCs. As expected, there was drug resistance across all GSC lines, with the immortalized U87 cell line demonstrating much higher sensitivity to chemotherapeutics, with 77% of drugs inducing 75% cell death or more. Recurrent GSC lines TD2 and TS9, for which the patient had previously been exposed to irradiation and TMZ, were highly resistant—with 34.5% and 13.5%, respectively, of drugs causing cell death at 75% or above (Supplementary File 1). Although there were GSC cell lines that were more resistant without prior exposure to chemotherapy, drugs that showed consistent cell death across all cell lines were rare, with only ACTD, bortezomib, and paclitaxel having a cytotoxic effect on every line.

Actinomycin D Induces Cell Death at Low Concentrations In Vitro, Inhibiting Self-Renewal, Invasion, and Migration

Drugs that inhibited cell viability by more than 75% were ranked, and the 12 most potent drugs acting on each cell line taken forward for 6-point dose response analysis. Not all drugs tested generated an IC_{50} in all cell lines. Drugs that produced a dose-response curve in at least 3 cell lines with no ambiguity are shown in Supplementary Figure 2. All IC_{50} data generated, plus 95% CIs, are reported in Supplementary Data File 1. We chose to test only paclitaxel and ACTD in our dose-response studies, as bortezomib has been tested in clinical trials and shown to penetrate and accumulate in GBM tumors without any antitumor effect, suggesting that alternative pathways in the tumor microenvironment are activated to protect neoplastic cells when systemic bortezomib is administered.[21] Paclitaxel has shown a modest effect in recurrent GBM, with 35% ($n = 41$) of patients showing disease stabilization or better[22]; however, in our dose-response studies, only 4 of our 12 cell lines were sensitive to paclitaxel. ACTD was the only drug tested in dose response which generated IC_{50} values in all cell lines. As ACTD has not previously been investigated in the clinic for GBM, we decided to focus any further investigations on validating ACTD effect in more detail.

Further in vitro studies showed that primary mixed mouse astrocytes demonstrate a higher tolerance to ACTD compared with GSC lines, with an IC_{50} of 28 μM, whereas in mouse neural stem cells, the IC_{50} is a considerably lower 7.2 μM (Fig. 1C). We also demonstrate that an increase of ACTD concentration leads to a corresponding increase in apoptosis through activation of caspase-3/7 in mouse NSCs and both recurrent GSC lines (Fig. 1D). We also investigated invasion in the 2 recurrent spheroid models

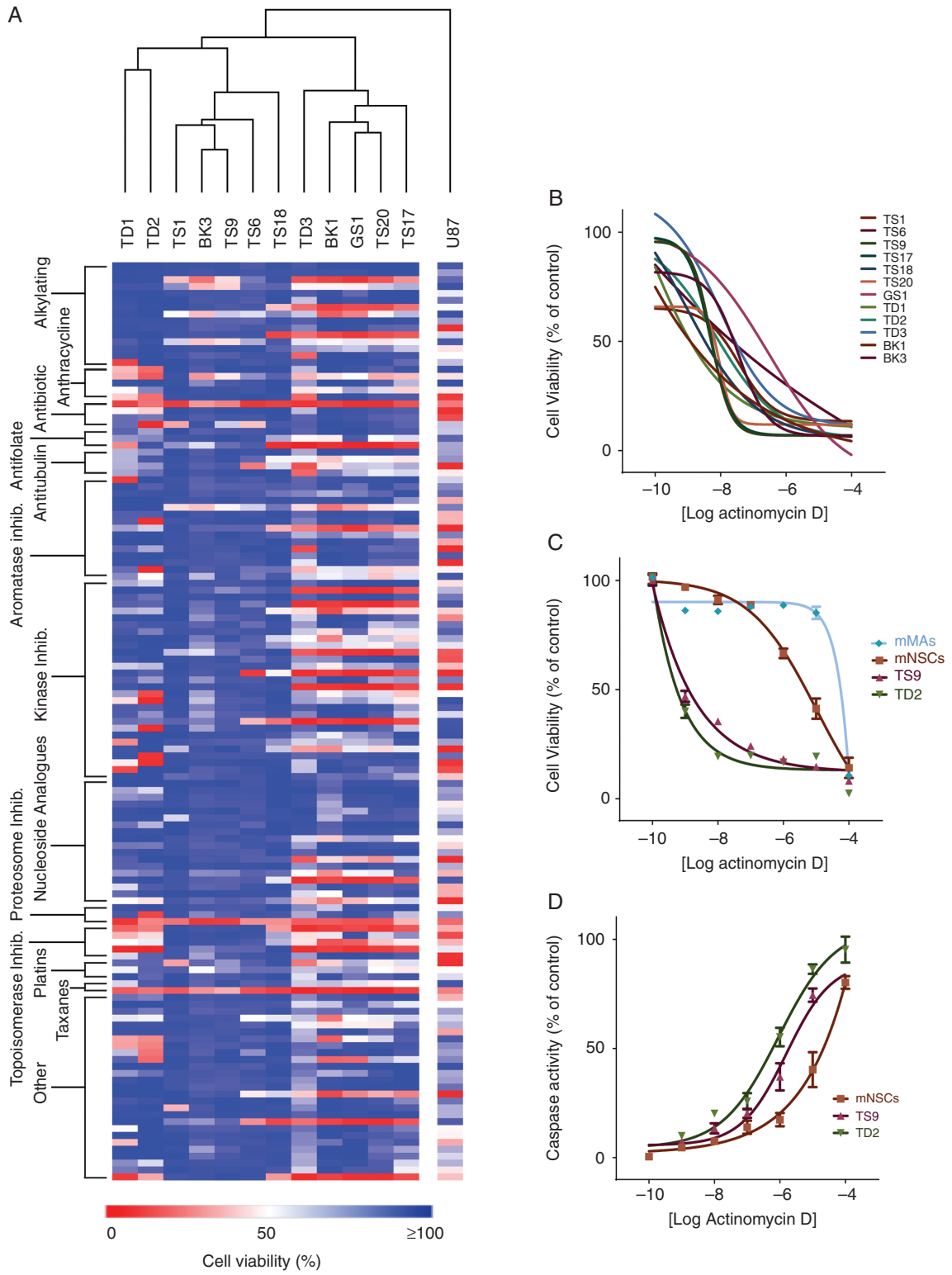

Fig. 1 (A) Heat map generated from the single shot 10 μM PrestoBlue viability screen. Data shown are the mean cell viability from duplicate wells from 2 separate runs. Rows are stacked by drug class and columns clustered by Euclidean distance. (B) Dose-response data for all patient-derived GSCs generated with ACTD in a 6-point dose response. (C) Mouse mixed astrocytes and mouse neural stem cells were compared with recurrent GSC lines to assess ACTD chemotoxicity. Data shown are the mean percent viability of 6 replicates per dose ± SD compared with controls. (D) Caspase-3/7 activation in mouse neural stem cells and recurrent GSC lines. Data shown are the mean fluorescence of 6 replicates per dose ± SD as a percentage of the positive staurosporine control.

TD2 and TS9 to assess the capability of ACTD to inhibit invasion, as well as proliferation. In both recurrent spheroid models, when ACTD was added to Matrigel, invasion decreased to approximately 70% and 50% at IC_{25}. At IC_{50}, invasion into Matrigel was reduced to just 9.9% in TS9 cells and 27% in TD2 cells (Fig. 2A, B). Finally, in a limiting dilution spheroid assay, we show that spheroid recovery and secondary sphere generation were inhibited significantly ($P < 0.0001$) by ACTD compared with vehicle and TMZ-treated spheroids.

Actinomycin D Reduces Tumor Volume in a Subcutaneous Model of Recurrent GBM

To first assess drug effect in vivo without the possible confounding effect on drug penetration of the blood–brain barrier, we tested ACTD in a subcutaneous model. After subcutaneous implantation of the recurrent GSC line TS9, mice were randomized to treatment. Vehicle-treated tumors grew on average from 200 mm^3 to over 700 mm^3, whereas in animals treated with ACTD, tumor volume

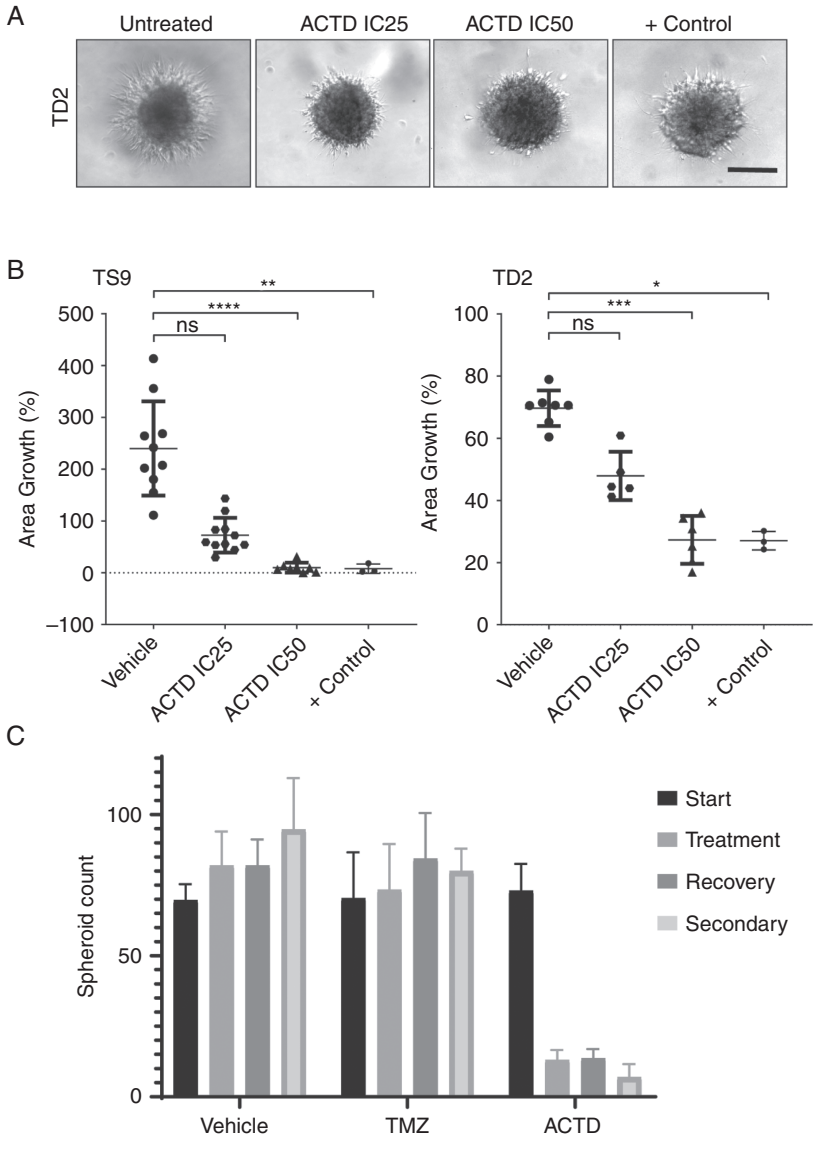

Fig. 2 (A) Cultured TS9 and TD2 GSC spheroids were embedded into Matrigel ± ACTD for 4 days. Representative images of TD2 from 4 days posttreatment with vehicle and low- and high-dose ACTD. Scale bar, 50 microns. (B) Quantification of the change in area of invasion compared with controls. Data shown are the mean invasion of 6 replicates per treatment ± SD as a percentage of vehicle-treated controls (*$P < 0.05$, **$P < 0.01$, ***$P < 0.001$, and **** $P < 0.0001$). (C) Recurrent GSC spheroids were treated with either DMSO, ACTD (IC_{50}), or TMZ (50 μM) for 4 days. Spheroids over 50 μm in diameter were counted, then plates were left to recover for 5 days. After counting, spheroids were dissociated and cells were reseeded. Secondary spheroid formation was assessed a further 5 days later. Data shown are the mean of 4 replicates ± SD. Number of spheroids at treatment stage—vehicle vs TMZ nonsignificant, vehicle vs ACTD ****$P < 0.0001$. Number of spheroids at secondary stage—vehicle vs TMZ nonsignificant, vehicle vs ACTD ****$P < 0.0001$.

was significantly reduced to an average of 85 mm^3, approximately 11% of control ($P < 0.0001$) (Fig. 3A). Animals treated with TMZ also had a slight significant reduction in tumor volume ($P = 0.0380$). Kaplan–Meier analysis was generated based on survival from initiation of treatment to humane endpoint. ACTD treatment had a significant effect on survival in this model ($P = 0.0322$) with no ACTD-treated animal reaching endpoint by the conclusion of the planned treatment schedule (Fig. 3B).

Actinomycin D Reduces Tumor Growth in Orthotopic Models of GBM

A puromycin-resistant, luciferase-expressing population of the recurrent TD2 patient-derived line was injected orthotopically into the right striatum of NSG mice. Based on pilot studies (Supplementary Figures 3–4), mice were imaged for bioluminescent signal at 6 weeks post-injection before randomization to treatment. Mice were dosed over

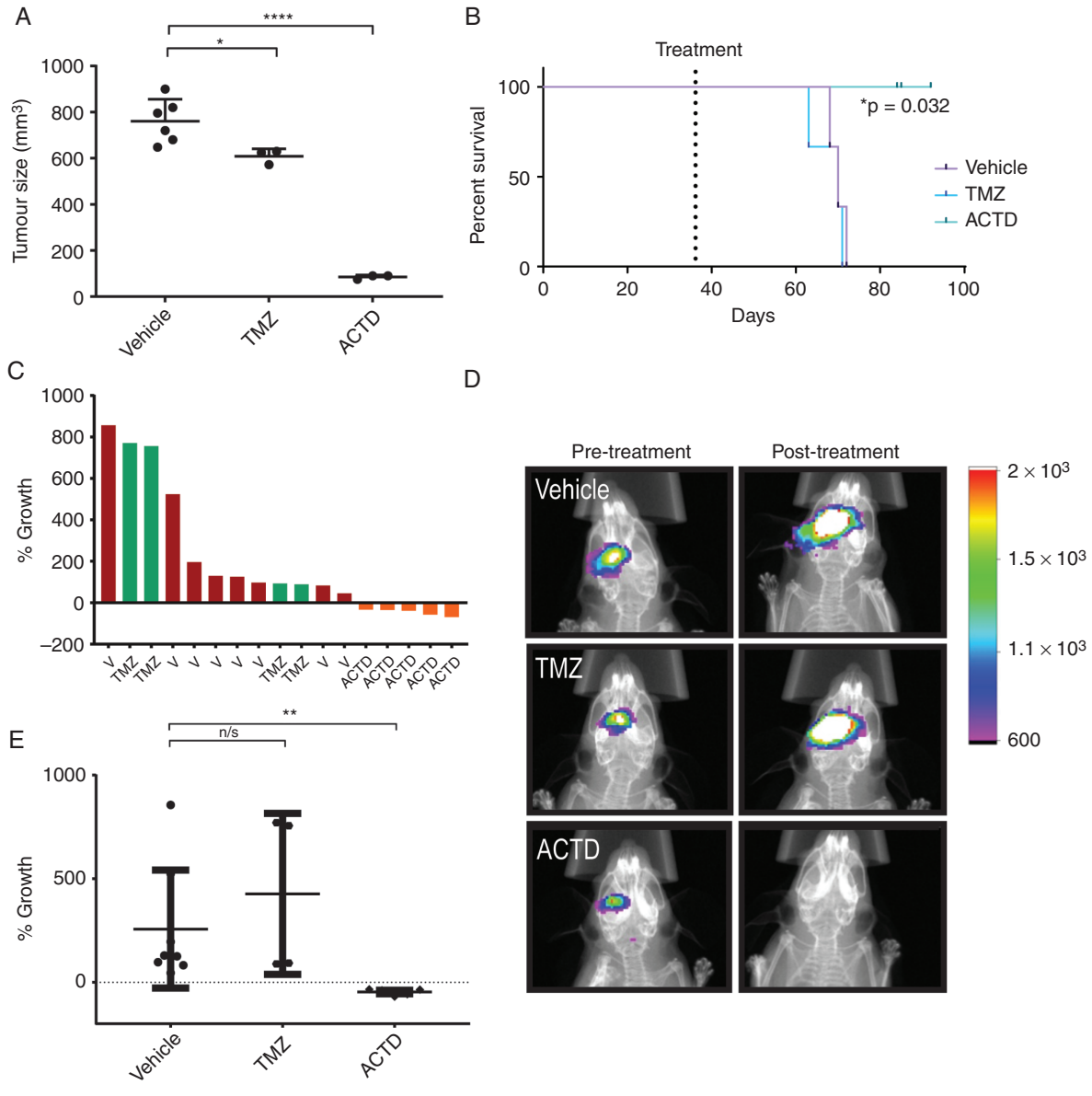

Fig. 3 (A, B) Subcutaneous in vivo validation of ACTD in patient-derived TS9 tumors. (A) Subcutaneous tumors were excised and measured ex vivo for accuracy, data shown are the volume of vehicle-, TMZ- and ACTD-treated subcutaneous tumors as measured by calipers (mm^3). Volume measurements were analyzed by one-way ANOVA and Tukey's multiple comparisons test. Significance = *$P < 0.05$, **$P < 0.01$, ***$P < 0.001$, and ****$P < 0.0001$. (B) Kaplan–Meier plots analyzing mouse survival between treatment groups; vehicle vs ACTD *$P = 0.032$. (C–E) Orthotopic in vivo validation of ACTD in patient-derived TD2 tumors. (C) Waterfall plot generated from all TD2 replicates demonstrates the change in tumor growth as a percent of the mean bioluminescent signal of vehicle-treated mice. (D) Representative images of bioluminescence from vehicle, TMZ, and ACTD-treated mice (legend = Average photons/sec/mm^2). (E) Percentage growth change (% growth) was tested by one-way ANOVA and Tukey's multiple comparison tests. Significance = *$P < 0.05$, **$P < 0.01$, ***$P < 0.001$, and ****$P < 0.0001$.

2 weeks, prior to reimaging at 8 weeks post-injection to assess tumor growth. ACTD significantly reduced tumor growth ($P = 0.0125$), while TMZ treatment had no significant effect on tumor growth during treatment ($P > 0.9999$) (Fig. 3C–E).

To assess long-term effects of ACTD treatment, the TD2 patient-derived line was implanted into a cohort of 25 mice for survival analysis (Fig. 4A). Treatment with high dose (0.1 mg/kg) ACTD yielded a significant increase in median survival from 62 days in both untreated and vehicle-treated mice to 79 days post-implant ($P = 0.0005$). Temozolomide treatment returned no significant survival benefit, with a median survival of 58 days. Interestingly, low dose ACTD-treated (0.05 mg/kg) mice also had a significant median survival of 92 days post-implant ($P = 0.0052$); however, one mouse in this treatment cohort had to be culled at 42 days due to an adverse reaction to the pen used for marking, and was excluded. A second demonstrated excessive circling and was culled at 40 days, which may or may not have been tumor related. This mouse was included. Three surviving ACTD mice remained at the end of the study period.

Histological analysis of tumor tissue showed that vehicle-treated mice had a larger number of hypertrophic astrocytes infiltrating the tumor, while vehicle- and TMZ-treated mice had significantly higher expression of the

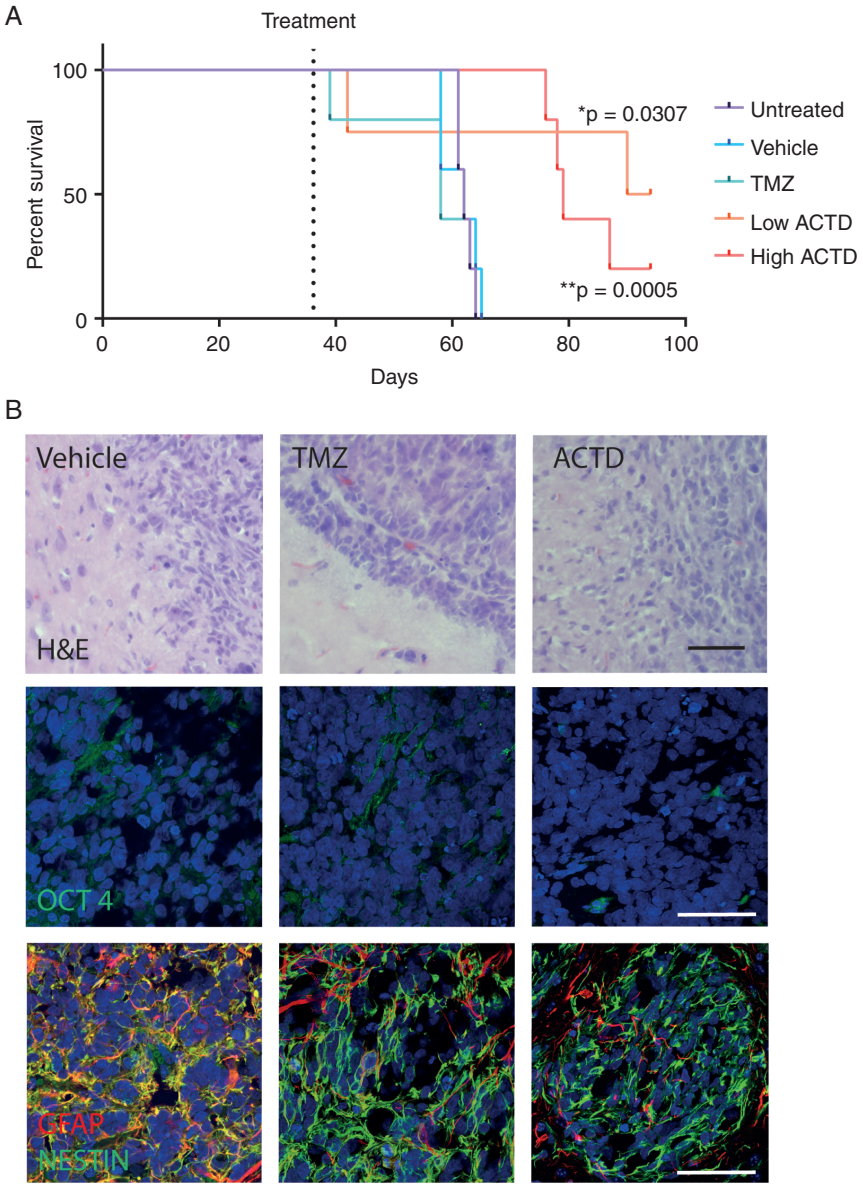

Fig. 4 (A) Kaplan–Meier plots analyzing mouse survival between treatment groups; vehicle vs TMZ nonsignificant, vehicle vs high dose ACTD (0.1 mg/kg) ***$P = 0.0005$; vehicle vs low dose ACTD (0.05 mg/kg) *$P = 0.0052$. (B) Representative images from the histological analysis of survival cohort treatment groups. Scale bars, 100 microns.

stem cell marker Oct4 within the tumor ($P = 0.0052$) than ACTD-treated mice (Fig. 4B (quantification data shown in Supplementary Figure 5). Results from quantitative reverse transcription PCR confirmed that ACTD-treated tumor cells from both TS9 and TD2 patient-derived models had significantly lower expression of Oct4 at the mRNA level, along with 3 other putative stem cell markers: Nanog, c-Myc, and Sox2 (Supplementary Figures 6–7).

Actinomycin D Downregulates Sox2 in Preclinical Models of GBM

Along with a demonstrable effect on cell viability, we saw that Sox2 expression decreased significantly in all our spheroid models after 48 hours exposure to low dose ACTD (Fig. 5A–D). When ACTD-treated spheroids were stained via immunocytochemistry and quantified, Sox2 was downregulated in TS9 cells by 65% and in TD2 cells by 80%. Western blots confirm Sox2 was downregulated in TS9 and TD2 cell lysates by 47% and 68%, respectively (Fig. 5B), suggesting that ACTD may be able to specifically target stemlike Sox2-expressing cells.

In excised TS9 subcutaneous tumors and TD2 orthotopic brain sections, Sox2 expression was also significantly downregulated in ACTD-treated mice compared with vehicle- and TMZ-treated mice (Fig. 5E–H). In TS9 tumors, ACTD-treated tumor expression of Sox2 was 1.93% of controls and in the orthotopic TD2 model, ACTD-treated Sox2 expression was just 0.3% of controls (Fig. 5F).

In a fourth in vivo study, a small cohort of mice were injected with TD2 cells and had ACTD delivered only once to increase the likelihood of available tumor tissue (Supplementary Figure 8). Western blot analysis of the 3 mice per group demonstrates that all mice had a significant reduction in Sox2 protein expression compared with vehicle-treated controls when normalized to α-tubulin. These data all suggest that ACTD has a specific Sox2 downregulation effect or preferential killing of Sox2-expressing cells in vivo.

Discussion

Despite an increased knowledge of the molecular and genetic pathogenesis of GBM, there are still limited treatment options available for patients at tumor recurrence. In this study, we demonstrate a validated HTS assay using patient-derived multicellular GSCs that can generate consistent, reproducible, and cost-effective drug sensitivity data on patient samples in a physiologically relevant format. Our assay highlights the intratumoral heterogeneity of GBM tumors seen in the clinic and the inherent resistance to standard chemotherapeutics that treatment-naïve patients can present with. This approach identifies patient-specific sensitivities to FDA-approved compounds that could impact clinic decision making in a personalized, informative way. Our HTS found that ACTD had a broad cytotoxic effect in all our screened cell lines. To the best of our knowledge, ACTD has not been trialed in GBM or recurrent GBM, nor has it been studied in orthotopic models of adult brain tumors. Due to the lack of standard of care in recurrent GBM, we chose to explore the efficacy of ACTD in recurrent models of GBM.

Our preclinical study of ACTD demonstrates that not only is ACTD highly effective in recurrent GBM mouse models, it is well tolerated by nonneoplastic differentiated mouse cells, both in vitro and in vivo. In cultured mouse mixed astrocytes, we see a dramatic increase in the drug concentration necessary for 50% cell death, while histology in the orthotopic model reveals a reduced number of hypertrophic glia in ACTD-treated mice (Fig. 4B). Additionally, mice tolerated drug treatment well, with no significant difference between weight change in ACTD-treated mice in TD2 tumor-bearing mice compared with vehicle-treated groups (Supplementary Figure 9). The efficacy of ACTD in orthotopic models also demonstrates that, in our hands, ACTD crosses the blood–brain barrier in vivo. Previous pharmacokinetic studies of ACTD indicate poor CNS penetration and uptake in the brain[23]; however, surgical and radiological studies have shown that the blood–brain barrier is disrupted to some extent in the majority of patients with GBM.[24] This suggests there could be many drugs previously thought to be ineffectual in brain tumors that could have potential for GBM, despite not easily passing through an intact blood–brain barrier. Olaparib, for example, is unable to penetrate the blood–brain barrier in healthy preclinical mouse models, yet was found to accumulate in 98.65% of both core and margin specimens from patients with recurrent GBM.[25]

There are many factors that contribute to the failure of treatments to dramatically improve survival for GBM over the last decade.[26] One mechanism that is believed to be largely responsible for resistance to treatment, and tumor recurrence, is the presence of a population of cancer stemlike cells that escape surgical intervention. Hägerstrand et al have previously demonstrated that a subset of highly tumorigenic cells from 20 GBM patients were Sox2 dependent, with an increased ability to form neurospheres and self-renew.[27] The group also found that this Sox2-dependent phenotype had a specific sensitivity to combination tyrosine kinase inhibitors, demonstrating the feasibility of stem cell–targeting therapies in the clinic. Our preclinical study offers robust evidence of efficacy of ACTD in 2 recurrent GBM mouse models, demonstrating significant survival benefit compared with rechallenge of TMZ. We discovered, through methylation subgrouping, that both our recurrent tumor models were derived from O^6-methylguanine-DNA methyltransferase (MGMT) unmethylated patients (Supplementary Data File 1). Overexpression of MGMT is associated with poor prognosis and often confers resistance to TMZ,[28,29] which is reflected in the response seen in our datasets to TMZ treatment. While 7 ACTD-treated mice did eventually succumb to disease, ACTD-treated tumors had a significant decrease in Sox2 and Oct4 protein. In addition, mRNA levels of Sox2, Oct4, Nanog, and c-Myc were significantly downregulated in cells from both patient-derived models.

Sox2 is necessary for the regulation of a complex network of transcription factors that affect expression of Oct4,[30] with both Oct4 and Sox2 shown to be implicated in the regulation of Nanog.[31] Chen et al have also previously demonstrated that c-Myc downregulation follows silencing of the Sox2 gene using short hairpin RNA.[32]

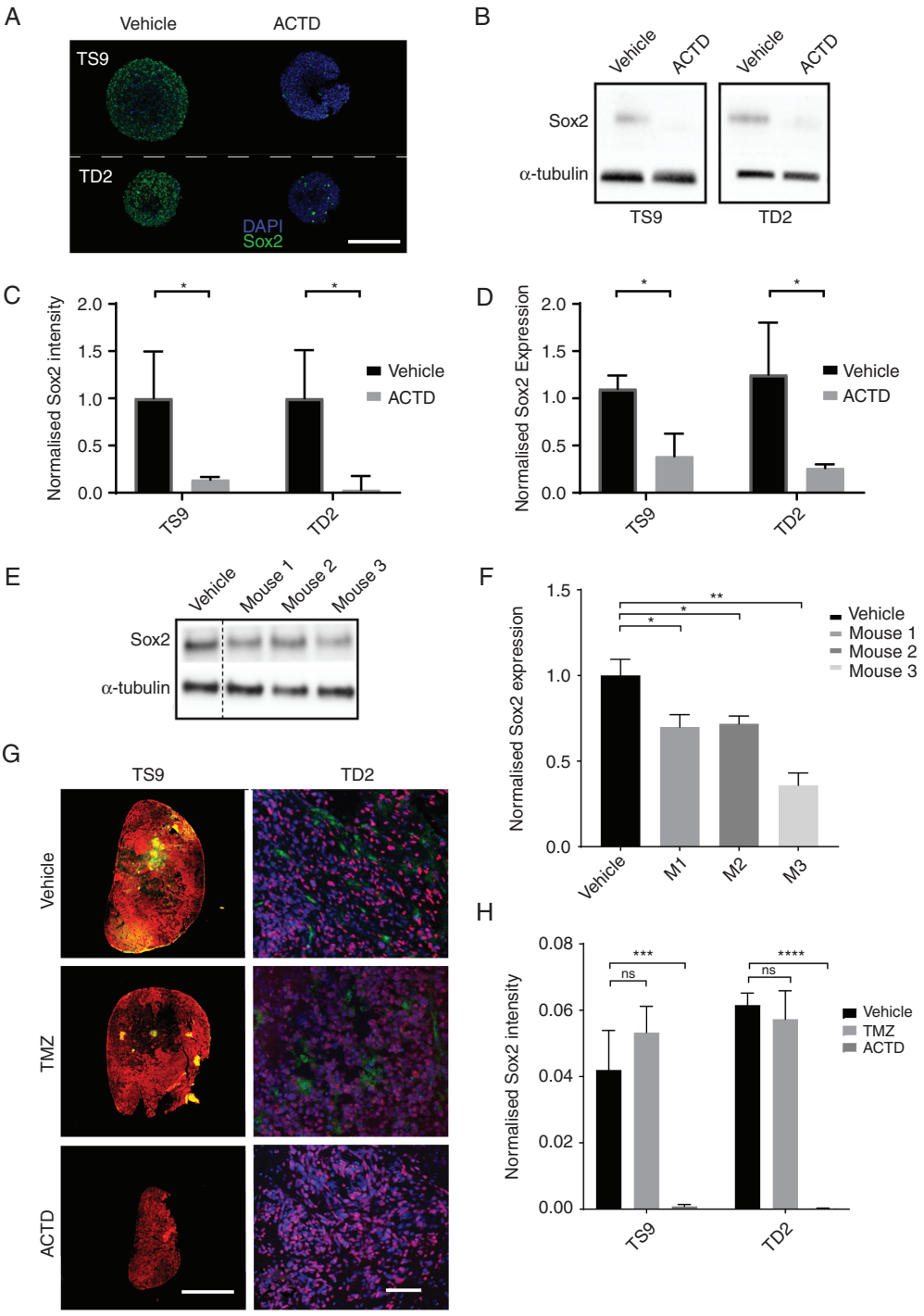

Fig. 5 (A–D) In vitro assessment of Sox2 downregulation. (A) Representative images of Sox2 whole spheroid immunocytochemistry. Scale bar, 200 microns. (B) Western blot for Sox2 and α-tubulin from ACTD-treated TS9 and TD2 cell lines. (C) Quantification of anti-Sox2 staining normalized to DAPI. Data shown are the mean of 3 replicates per cell line ± SD. (D) Quantification analysis of Sox2 western blots. Values represent mean Sox2 expression of cells normalized to α-tubulin, relative to nontreated control ($n = 2$). (E–H) In vivo assessment of Sox2 downregulation. (E) Western blot of tumor hemisphere homogenate from three TD2 tumor-bearing mice. Lysates were probed for Sox2 and α-tubulin expression. (F) Quantification analysis of Sox2 in vivo western blots ($n = 3$). Lysate from 3 mice was tested in triplicate and Sox2 expression normalized to α-tubulin. Data shown are the mean from each western blot experiment for each mouse relative to vehicle-treated mice ($n = 3$). Significance = $^{*}P < 0.05$, $^{**}P < 0.01$, $^{***}P < 0.001$, and $^{****}P < 0.0001$. (G) Representative immunofluorescence staining of Nestin and Sox2 in TS9 tumors and Ki67 and Sox2 staining in TD2 survival cohort tumors. Scale bars, 200 microns. Anti-Sox2 staining quantified and normalized to Nestin (TS9) or DAPI (TD2). Data shown are the mean of 3 mice per treatment ± SD.

Therefore, our data strongly suggest that the survival benefit of ACTD is due to a specific downregulation of the transcription factor Sox2. ACTD binds strongly at guanine, and Sox2 has guanine-cytosine–rich 18 base pair sequences in the promoter region.[33,34] This preferential binding of ACTD to guanine-cytosine–rich sites would explain the downregulation of Sox2 protein expression in our models. Significantly, ACTD has also been successful in the clinic as part of combination therapy for Ewing sarcoma, in which Sox2 has been demonstrated to have a fundamental role in growth and survival.[35] Das et al have also recently shown that ACTD suppresses Sox2 at the transcriptional level, leading to the decrease in protein expression that we also see in our models.[36]

Interestingly, while we see an upregulation in apoptosis at high concentrations in our in vitro models, we also see a decrease in migration even at very low concentrations of ACTD. Additionally, mice treated with low dose ACTD had a higher median survival rate of 92 days, compared with just 62 days for vehicle-treated mice and 79 days for high dose ACTD. Low dose ACTD has recently been shown to restore p53 function in ependymoma positive for RELA (v-rel avian reticuloendotheliosis viral oncogene homolog A).[37] ACTD stabilizes p53 through the disruption of ribosome biogenesis, which redirects the RPL5/RPL11/5S rRNA pre-ribosomal complex to human double minute 2 homolog inhibition.[38] However, Cortes et al have found that low concentrations can also induce cell death in p53-deficient neuroblastomas, indicating an alternative p53-independent mechanism.[39]

Our recurrent GBM experimental models are based on undifferentiated GSCs that were amenable to culture post biopsy. Although we are confident that our in vivo models reflect the methylation subgroup of the original tumor tissue (Supplementary Data File 1), it is likely that there are other cells present within the tumor bulk that harbor various, unobservable, and potentially resistant phenotypes. The heterogeneous nature of GBM necessitates a multimodal approach, especially at recurrence, and this study indicates that ACTD could be a useful addition to second-line therapy, enabling targeting of both the stem- and nonstem cell components of the tumor mass. ACTD has previously been demonstrated by Valeriote et al[40] to have a dose-dependent, cycle-specific cytotoxicity effect on cells, killing proliferating neoplastic cells effectively at low doses while having a cytotoxic effect on leukemia stem cells through accumulation. In agreement with this observation, in our models we see a large initial decrease in tumor bulk, alongside a more long-term reduction in stemness markers.

Treatment at diagnosis with TMZ has been shown to induce a hypermutated recurrent phenotype, with specific driver mutations in the Akt–mammalian target of rapamycin and retinoblastoma pathways that are known to be induced by TMZ.[41] Fractionated radiotherapy can also induce accelerated driver mutations in radioresistant cell populations in the tumor mass.[42] Moreover, in vivo microRNA inhibition of Sox2 and Oct4 has been demonstrated to increase survival in an orthotopic patient-derived model of GBM when used in conjunction with radiotherapy and TMZ,[43] while overexpression of Sox2 has been shown to enhance the expression of the multidrug-resistant protein ABCC3 (ATP-binding cassette subfamily C member 3), which is overexpressed in human GBM at both the mRNA and the protein level.[44] Thus, ACTD may also be a potential adjuvant to first-line therapy to reduce TMZ resistance and target stem cell populations post surgical intervention.

It must be noted, however, that ACTD has been shown to potentiate radiotherapy effects posttreatment, thus some adverse effects may arise in patients who have had previous radiotherapy, or if ACTD was to be trialed in patients receiving ACTD as an adjuvant to the Stupp protocol. D'Angio et al first described effects of combination ACTD with radiotherapy in the 1950s, publishing evidence that skin erythema appeared earlier than usual and at a much lower dose than expected.[45] This implies that ACTD could accentuate the effect of radiation, yet there is to our knowledge no evidence of combination radiotherapy and ACTD in the brain. Preclinical in vivo studies that include radiotherapy would therefore be a must before ACTD was considered for first-line therapy, where targeted radiation is common. Despite this, our preclinical data strongly support the use of ACTD in the clinic for second-line therapy.

In conclusion, we have demonstrated that in multiple models of GBM, ACTD treatment significantly inhibits tumor growth and increases survival and that this is accompanied by a measurable decrease in Sox2-positive GSCs. Based on the current lack of options for relapsed GBM patients and the FDA-approval status of ACTD, we believe this study warrants further exploration of ACTD efficacy in a clinical setting.

Supplementary Material

Supplementary data are available at *Neuro-Oncology* online.

Keywords

actinomycin D | drug repurposing | glioblastoma multiforme | high throughput screening | preclinical studies

Funding

JTT and BWB received grant funding from the Christie Charitable Fund. The Bioimaging Facility microscopes used in this study were purchased with grants from BBSRC, Wellcome, and the University of Manchester Strategic Fund.

Conflict of interest statement. None declared.

Acknowledgments

We gratefully acknowledge the support and clinical insight given by Professor Richard J. Gilbertson, the help and assistance of the staff of the Biological Sciences Facility, the Bioimaging Facility at the University of Manchester, and Alan Mackay and the rest of the Glioma Team at the Institute for Cancer Research, London.

Authorship statement. Conceived, designed, and carried out all experiments, analyzed the data, generated the figures, and wrote the paper JTT. Assisted with experiments and contributed to analysis SE, SW, AP. Assisted with experiments GF, EN, HP. Assisted with immunocytochemical experiments CAW. Assisted with automation and analysis of image sets EZ. Facilitated the use of the screening platform and assisted with automation and liquid handling ME. Facilitated the use of the screening platform and assisted with automated assay design AD. Facilitated in vivo experiments, provided training and expertise KJW. Provided clinical insights, reviewed data and paper, MM, CM. Conceived the initial project, designed experiments, and reviewed data and paper BWB

References

1. Cancer Genome Atlas Research Network. Comprehensive genomic characterization defines human glioblastoma genes and core pathways. *Nature.* 2008; 455(7216):1061–1068.
2. Stupp R, Mason WP, van den Bent MJ, et al. Radiotherapy plus concomitant and adjuvant temozolomide for glioblastoma. *N Engl J Med.* 2005; 352(10):987–996.
3. Palmer JD, Bhamidipati D, Song A, et al. Bevacizumab and re-irradiation for recurrent high grade gliomas: does sequence matter? *J Neurooncol.* 2018;140(3):623–628.
4. Wong CH, Siah KW, Lo AW. Estimation of clinical trial success rates and related parameters [published correction appears in Biostatistics. 2019 Apr 1;20(2):366]. *Biostatistics.* 2019;20(2):273–286.
5. Guerra-Rebollo M, Garrido C, Sánchez-Cid L, et al. Targeting of replicating CD133 and OCT4/SOX2 expressing glioma stem cells selects a cell population that reinitiates tumors upon release of therapeutic pressure. *Sci Rep.* 2019;9(1):9549.
6. Neradil J, Veselska R. Nestin as a marker of cancer stem cells. *Cancer Sci.* 2015;106(7):803–811.
7. de la Rocha AM, Sampron N, Alonso MM, Matheu A. Role of SOX family of transcription factors in central nervous system tumors. *Am J Cancer Res.* 2014; 4(4):312–324.
8. Lee JH, Lee JE, Kahng JY, et al. Human glioblastoma arises from subventricular zone cells with low-level driver mutations. *Nature.* 2018;560(7717):243–247.
9. Auffinger B, Tobias AL, Han Y, et al. Conversion of differentiated cancer cells into cancer stem-like cells in a glioblastoma model after primary chemotherapy. *Cell Death Differ.* 2014;21(7):1119–1131.
10. Biddle A, Gammon L, Liang X, Costea DE, Mackenzie IC. Phenotypic plasticity determines cancer stem cell therapeutic resistance in oral squamous cell carcinoma. *EBioMedicine.* 2016;4:138–145.
11. Uwanogho D, Rex M, Cartwright EJ, et al. Embryonic expression of the chicken Sox2, Sox3 and Sox11 genes suggests an interactive role in neuronal development. *Mech Dev.* 1995;49(1-2):23–36.
12. Ben-Porath I, Thomson MW, Carey VJ, et al. An embryonic stem cell-like gene expression signature in poorly differentiated aggressive human tumors. *Nat Genet.* 2008;40(5):499–507.
13. Liu K, Lin B, Zhao M, et al. The multiple roles for Sox2 in stem cell maintenance and tumorigenesis. *Cell Signal.* 2013;25(5):1264–1271.
14. Sathyan P, Zinn PO, Marisetty AL, et al. Mir-21-Sox2 axis delineates glioblastoma subtypes with prognostic impact. *J Neurosci.* 2015;35(45):15097–15112.
15. Gangemi RM, Griffero F, Marubbi D, et al. SOX2 silencing in glioblastoma tumor-initiating cells causes stop of proliferation and loss of tumorigenicity. *Stem Cells.* 2009;27(1):40–48.
16. Yu KK, Taylor JT, Pathmanaban ON, et al. High content screening of patient-derived cell lines highlights the potential of non-standard chemotherapeutic agents for the treatment of glioblastoma. *PLoS One.* 2018;13(3):e0193694.
17. Capper D, Jones DTW, Sill M, et al. DNA methylation-based classification of central nervous system tumours. *Nature.* 2018;555(7697):469–474.
18. Campeau E, Ruhl VE, Rodier F, et al. A versatile viral system for expression and depletion of proteins in mammalian cells. *PLoS One.* 2009;4(8):e6529.
19. Sergijenko A, Langford-Smith A, Liao AY, et al. Myeloid/microglial driven autologous hematopoietic stem cell gene therapy corrects a neuronopathic lysosomal disease. *Mol Ther.* 2013;21(10):1938–1949.
20. Zhang JH, Chung TD, Oldenburg KR. A simple statistical parameter for use in evaluation and validation of high throughput screening assays. *J Biomol Screen.* 1999;4(2):67–73.
21. Raizer JJ, Chandler JP, Ferrarese R, et al. A phase II trial evaluating the effects and intra-tumoral penetration of bortezomib in patients with recurrent malignant gliomas. *J Neurooncol.* 2016;129(1):139–146.
22. Prados MD, Schold SC, Spence AM, et al. Phase II study of paclitaxel in patients with recurrent malignant glioma. *J Clin Oncol.* 1996;14(8):2316–2321.
23. Walsh C, Bonner JJ, Johnson TN, et al. Development of a physiologically based pharmacokinetic model of actinomycin D in children with cancer. *Br J Clin Pharmacol.* 2016;81(5):989–998.
24. Oberoi RK, Parrish KE, Sio TT, Mittapalli RK, Elmquist WF, Sarkaria JN. Strategies to improve delivery of anticancer drugs across the blood-brain barrier to treat glioblastoma. *Neuro Oncol.* 2016;18(1):27–36.
25. Halford SER, Cruickshank G, Dunn L, et al. Results of the OPARATIC trial: a phase I dose escalation study of olaparib in combination with temozolomide (TMZ) in patients with relapsed glioblastoma (GBM). *J Clin Oncol.* 2017; 35(15_suppl):2022–2022.
26. Ho VK, Reijneveld JC, Enting RH, et al; Dutch Society for Neuro-Oncology (LWNO). Changing incidence and improved survival of gliomas. *Eur J Cancer.* 2014;50(13):2309–2318.
27. Hägerstrand D, He X, Bradic Lindh M, et al. Identification of a SOX2-dependent subset of tumor- and sphere-forming glioblastoma cells with a distinct tyrosine kinase inhibitor sensitivity profile. *Neuro Oncol.* 2011;13(11):1178–1191.
28. Taylor JW, Schiff D. Treatment considerations for MGMT-unmethylated glioblastoma. *Curr Neurol Neurosci Rep.* 2015;15(1):507.
29. Pandith AA, Qasim I, Zahoor W, et al. Concordant association validates MGMT methylation and protein expression as favorable prognostic factors in glioma patients on alkylating chemotherapy (temozolomide). *Sci Rep.* 2018;8(1):6704.
30. Masui S, Nakatake Y, Toyooka Y, et al. Pluripotency governed by Sox2 via regulation of Oct3/4 expression in mouse embryonic stem cells. *Nat Cell Biol.* 2007;9(6):625–635.
31. Rodda DJ, Chew JL, Lim LH, et al. Transcriptional regulation of nanog by OCT4 and SOX2. *J Biol Chem.* 2005;280(26):24731–24737.

32. Chen S, Xu Y, Chen Y, et al. SOX2 gene regulates the transcriptional network of oncogenes and affects tumorigenesis of human lung cancer cells. *PLoS One.* 2012;7(5):e36326.
33. Bailly C, Kluza J, Martin C, Ellis T, Waring MJ. DNase I footprinting of small molecule binding sites on DNA. *Methods Mol Biol.* 2005;288:319–342.
34. Grimmer MR, Stolzenburg S, Ford E, Lister R, Blancafort P, Farnham PJ. Analysis of an artificial zinc finger epigenetic modulator: widespread binding but limited regulation. *Nucleic Acids Res.* 2014;42(16):10856–10868.
35. Ren C, Ren T, Yang K, et al. Inhibition of SOX2 induces cell apoptosis and G1/S arrest in Ewing's sarcoma through the PI3K/Akt pathway. *J Exp Clin Cancer Res.* 2016;35:44.
36. Das T, Nair RR, Green R, et al. Actinomycin D down-regulates SOX2 expression and induces death in breast cancer stem cells. *Anticancer Res.* 2017;37(4):1655–1663.
37. Tzaridis T, Milde T, Pajtler KW, et al. Low-dose actinomycin-D treatment re-establishes the tumoursuppressive function of P53 in RELA-positive ependymoma. *Oncotarget.* 2016;7(38):61860–61873.
38. Donati G, Peddigari S, Mercer CA, Thomas G. 5S ribosomal RNA is an essential component of a nascent ribosomal precursor complex that regulates the Hdm2-p53 checkpoint. *Cell Rep.* 2013;4(1):87–98.
39. Cortes CL, Veiga SR, Almacellas E, et al. Effect of low doses of actinomycin D on neuroblastoma cell lines. *Mol Cancer.* 2016;15:1.
40. Valeriote F, Vietti T, Tolen S. Kinetics of the lethal effect of actinomycin D on normal and leukemic cells. *Cancer Res.* 1973;33(11):2658–2661.
41. Johnson BE, Mazor T, Hong C, et al. Mutational analysis reveals the origin and therapy-driven evolution of recurrent glioma. *Science.* 2014;343(6167):189–193.
42. Kim SH, Yoo H, Chang JH, et al. Procarbazine and CCNU chemotherapy for recurrent glioblastoma with MGMT promoter methylation. *J Korean Med Sci.* 2018;33(24):e167.
43. Yang YP, Chien Y, Chiou GY, et al. Inhibition of cancer stem cell-like properties and reduced chemoradioresistance of glioblastoma using microRNA145 with cationic polyurethane-short branch PEI. *Biomaterials.* 2012;33(5):1462–1476.
44. Jeon HM, Sohn YW, Oh SY, et al. ID4 imparts chemoresistance and cancer stemness to glioma cells by derepressing miR-9*-mediated suppression of SOX2. *Cancer Res.* 2011;71(9):3410–3421.
45. D'Angio GJFS, Maddock CL. Potentiation of x-ray effects by actinomycin D. *Radiology.* 1959; 73:175–177.